A Nonequilibrium Model for Distillation Processes

Yin-Chun Liang, Zheng Zhou, You-Ting Wu, Jiao Geng, and Zhi-Bing Zhang
College of Chemistry and Chemical Engineering, Nanjing University, Nanjing, 210093, China

DOI 10.1002/aic.11037
Published online November 3, 2006 in Wiley InterScience (www.interscience.wiley.com).

A general thermodynamic model is developed by combining organically the nonequilibrium thermodynamic analysis with the traditional METSH simulation of distillation processes. The model is capable of both simulating industrial distillation processes and analyzing energy consumptions of the processes. The benzene–toluene binary distillation is selected as the model system to test the theory, and the industrial-scale tray column is studied in this work. The simulation results show that the tray structure and operation parameters have significantly influenced the entropy generation rate (EGR). It is also found that the development of vapor and liquid flow patterns on the industrial-scale trays can enhance tray efficiency and result in evident reduction of the EGR. The model is suitable for tray design, column performance analysis, and energy consumption evaluation of distillation processes. © 2006 American Institute of Chemical Engineers *AIChE J,* 52: 4229–4239, 2006
Keywords: distillation process, nonequilibrium thermodynamics, entropy generation rate

Introduction

The distillation process, taking energy as the only driving force, is a major energy consumption step in chemical process industries. It is of considerable importance to thermodynamically analyze the distillation process for the purpose of energy saving. There are four kinds of thermodynamic methods applied to the analysis of energy consumptions: the first law, second law, exergy, and nonequilibrium thermodynamic analyses. The first law of thermodynamics states the conservation of energy, whereas the second law provides information of energy efficiency. The exergy analysis, developed from the combination of the first law and the second law, is widely used nowadays for the design and analysis of thermal systems and provides an important and systematic method within the scope of equilibrium thermodynamics to diagnose whether and to what extent it is possible to reduce the inefficiency of a process. The magnitude of the inefficiency depends on the irreversibility of the process. The irreversibility may come from such phenomena fluid friction, heat transfer caused by finite temperature-driving forces, mass transfer caused by finite concentration or activity-driving forces, chemical reactions proceeding at finite displacements from chemical equilibrium, and mixing of streams under different conditions (temperature, pressure, and/or composition).[1]

Nonequilibrium thermodynamic analysis—also known as the third law of thermodynamic analysis—is a general theory used particularly for nonequilibrium processes. It systematically reveals the mechanism of entropy generation and shows the exact locations and reasons of exergy losses caused by the irreversible phenomena mentioned above. Nonequilibrium thermodynamic analysis is a powerful theoretical tool and has a tendency to implement and/or replace the exergy analysis. Recently, considerable advances have been made by applying nonequilibrium thermodynamics to analyze distillation processes.[2] Some attempts[3,4] were made to combine the distillation-process simulation with nonequilibrium thermodynamic analysis. However, quite a few methods presented in this specialized field could be applied directly to the practical design of distillation processes.

Correspondence concerning this article should be addressed to Z.-B. Zhang at segz@nju.edu.cn.

The focus of nonequilibrium thermodynamic analysis is to calculate the process entropy generation rate (EGR). Based on the assumption that the phenomenological transfer coefficient was constant and positive over the process, Tondeur and Kvaalen[5] found that a uniform distribution of the local EGR was optimal for reducing the total EGR. As an extension, Ratkje and Sauar[3] analyzed the effect of the distribution of heaters in a distillation column. They demonstrated that the EGR for a distillation column was at a minimum when the driving forces for separation were uniformly distributed along the column. Recently, Liu and Zhang[4] found that besides technological renovations of the whole process and various selections of operation parameters, the design of the tray structure could also significantly influence the EGR process. Based on this conclusion and theoretical calculations, a new energy-saving tray with optimized tray-structure parameters—the "95 tray"—was proposed and designed.

However, the majority of analysis models mentioned above were not suitable for evaluating the EGR of industrial-scale distillation columns because these models contained some systematic assumptions or simplifications that deviated from the real situations. For example, the EGR in the liquid phase was usually neglected; the liquid and vapor phases were assumed as completely mixed; and the tray efficiencies were postulated to be invariable.

The simulation of distillation processes was traditionally based on the ideal equilibrium stages. However, for a practical process the equilibrium condition could hardly be achieved so that the simulation results, based on the ideal equilibrium stages, largely strayed away from the real case. Models of nonequilibrium stages avoid the assumption of equilibrium and thus give more rigorous simulation. Such models are mainly divided into two categories: (1) the equilibrium stage–tray efficiency models and (2) the rate-based models.

In the equilibrium stage–tray efficiency models, a deviation is assumed to exist between the equilibrium stage and the actual stage. The tray efficiency is introduced to account for the deviation and the correlation of the tray efficiency is key to the models. Advances in multicomponent mass-transfer theory and developments of convenient matrix methods have led to more realistic stage models. These models were known as the multicomponent efficiency (MEF) stage model[6] in which efficiency matrices were used instead of component efficiencies. It is the main characteristic of the efficiency-based models that all references to the interface state are cancelled out by using the overall mass-transfer coefficient (K^{OV}). However, it should be pointed out that these efficiency-based models might predict incorrect mass-transfer directions, given that the interactions between the multicomponent mass-transfer rates[7] are usually neglected. Therefore, methods that take the interaction effects into account should be developed. Fortunately, some explicit solutions were recently proposed in the literature, such as those of Krishna[8] and Taylor and Smith,[9] that were expressed using a complicated formulation of the addition of resistances to account for the interactions between multicomponent mass-transfer rates. The solutions relied on two key assumptions: (1) the heats of vaporization were the same for all components and (2) the sensible heat terms in energy balance were negligible compared with latent heat terms. The first assumption can usually be avoided by using a new version of the addition of resistances formula, which is more complicated than those mentioned above, whereas the second assumption is still required.[6] In the literature,[11] several simulation experiments were carried out to find out how and when the inconsistency between the MEF model[6] and the nonequilibrium stage model (NEQ) model[7] appeared. It was observed that only the heaviest component was allowed to have a large relative deviation of mass flux in the range of diluted concentrations. The reason is that the diffusion flux of the diluted heaviest component itself was small and was calculated by subtracting all fluxes of other components from the total flux, being imposed with an accumulated deviation. For other components, the deviations of mass fluxes were typically $<5\%$, whereas the calculated vapor mole fractions of these components deviated from their actual values not $>0.5\%$. It is therefore expected that these solutions could be used to predict correct mass-transfer directions for most multicomponent distillation processes.

The rate-based models are alternative solutions that overcome the problem of predicting incorrect mass-transfer directions because the interactions between multicomponent mass-transfer rates are expressed in an implicit way. One of the most representative rate-based models is the NEQ stage model proposed by Krishnamuthy and Taylor.[7] In the model, the conservation equations were written separately for each phase and interface and then solved together with constitutive transport equations. Variables, such as tray efficiency and mass-transfer unit numbers, were avoided because they were difficult to be defined and confirmed. However, the mixed liquid and vapor phases were assumed in the NEQ model and the mole fractions were approximately estimated using arithmetic or logarithmic averages of the entering and exiting mole fractions. It was a simplified model for all but some small laboratory- and pilot-scale columns and was not a particularly accurate reflection of true flow patterns on a real distillation tray, as indicated by Kooijman and Taylor.[10] The KT (Kooijman and Taylor) model[10] and an overall rate-based (ORB) model[11] were thus developed to accurately simulate the temperature and composition gradients on industrial-scale trays. Compared to the efficiency-based models, the rate-based models are more accurate but more complicated.

In this work a general process simulation and energy analysis model is developed for industrial-scale distillation columns. The simulation is mainly based on the overall mass-transfer coefficient (K^{OV}) that is additionally used to calculate the process EGR in nonequilibrium thermodynamic analysis. The process simulation and energy analysis in the model are thus combined organically by using the overall mass-transfer coefficient as the bridging component.

The Framework of the Process Simulation and Energy Analysis Model

Our new model contains two aspects: the calculation of EGR and the simulation of distillation processes. In two aspects, the mass and heat transfers of the process are assumed to be at an irreversible thermodynamic state.

The model presented here is based on the well-known tray model as shown in Figure 1, in which the following assumptions are proposed:

(1) Steady-state conditions
(2) One-dimensional flow of vapor and liquid phases
(3) No significant pressure gradient along the gas and liquid flow directions
(4) The liquid is divided into a number of pools in series, with complete mixing of the liquid in each pool
(5) The vapor rising through the liquid pools is completely mixed

The Entropy Generation Rate on the Industrial-Scale Tray

The calculation of EGR per unit volume derived by Liu and Zhang[4] was rigorous for small trays because the assumption of complete mixing of the liquid and vapor phases was close to the real case. On industrial-scale trays (tray diameter > 0.8 m), there are significant temperature and composition gradients, and the assumption of complete mixing becomes nonrealistic. However, it is still reasonable to divide the liquid flowing on the tray into a series of pools with different temperatures and compositions, whereas in each pool the liquid and vapor phases are still assumed to be mixed completely, as shown in Figure 1.

The entropy generation rate per unit volume (σ) in a system of c species with no chemical reactions can be written as[12]

$$\sigma = -J_q \nabla\left(\frac{1}{T}\right) - \sum_{i=1}^{c} J_i \nabla\left(\frac{\mu_i}{T}\right) \tag{1}$$

For a distillation column separating a binary mixture, there are three fluxes across the vapor–liquid phase boundary: the heat flux J_q and two mass fluxes J_l and J_h. According to the Gibbs–Duhem equation, we have

$$\nabla\mu_h = -\frac{x_\ell}{x_h}\nabla\mu_\ell \tag{2}$$

By introducing Eq. 2 into Eq. 1, σ can be written as

$$\sigma = -J_q \frac{\nabla T}{T^2} - J_d \frac{x_\ell \nabla\mu_\ell}{T} \tag{3}$$

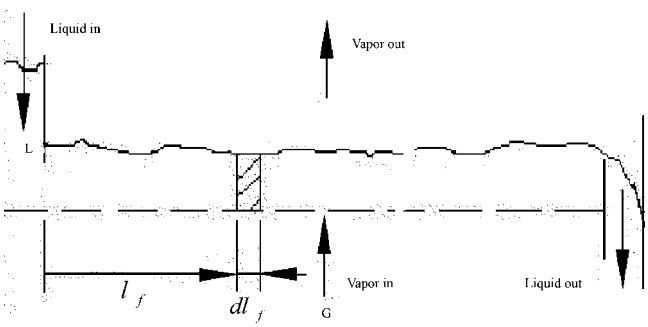

Figure 1. Vapor and liquid streams on a stage.

$$J_d = \frac{J_\ell}{x_\ell} - \frac{J_h}{x_h} \tag{4}$$

where J_d is the relative mass flux across the interface. According to the linear phenomenological relationship of nonequilibrium thermodynamics, these flux equations can be expressed by

$$J_q = -l_{qq}\frac{\nabla T}{T} - l_{q\ell}x_\ell \nabla\mu_\ell \tag{5}$$

$$J_d = -l_{\ell q}\frac{\nabla T}{T} - l_{\ell\ell}x_\ell \nabla\mu_\ell \tag{6}$$

By introducing Eq. 6 into Eq. 5, the heat flux can be expressed as

$$J_q = -\lambda\nabla T + \frac{l_{\ell q}}{l_{\ell\ell}}J_d \tag{7}$$

where

$$\lambda = \frac{\left(l_{qq} - l_{q\ell}\frac{l_{\ell q}}{l_{\ell\ell}}\right)}{T} \tag{8}$$

The EGR per unit volume is obtained by introducing Eq. 7 into Eq. 3:

$$\sigma = \lambda\left(\frac{\nabla T}{T}\right)^2 + \frac{{J_d}^2}{l_{\ell\ell}T} \tag{9a}$$

$$= \sigma_q + \sigma_\ell \tag{9b}$$

The first term on the righthand side of Eq. 9a is the EGR per unit volume arising from the temperature gradient σ_q and the second is the EGR per unit volume arising from mass transfer σ_l.

The total EGR resulting from mass separation for a pool, as shown in Figure 1, can be written as

$$\Theta_p = \int_v \sigma_\ell dv = \int_{v^l} \sigma_\ell dv + \int_{v-v^l} \sigma_\ell dv \tag{10}$$

where $v^l = a \times \Delta x$ is the volume of the interface, a is the interface area per froth volume, and Δx is the thickness of the interface film. According to the definition of the thermodynamic interface layer, there is no relative mass transfer in the bulks of the gas and liquid phases ($J_d \approx 0$), which implies

$$\int_{v-v^l} \sigma_\ell dv = 0 \tag{11}$$

Assuming $\bigtriangledown T \approx 0$ between two sides of the interface layer, l_{ll} can be obtained from Eq. 6:

$$l_{\ell\ell} = -\left(\frac{J_d}{x_\ell \nabla\mu_\ell}\right)_{\nabla T=0} \tag{12}$$

By introducing Eq. 11 and Eq. 12 into Eq. 10, and integrating over the transport path, we have

$$\Theta_p = \int -\frac{x_\ell \nabla \mu_\ell J_d}{T} dv = -\frac{x_\ell J_d}{T} a \int_0^{\Delta x} \nabla \mu_\ell \, dx \tag{13}$$

Because the value of $\bigtriangledown \mu_l$, the chemical potential gradient of the light component along transport path, can hardly be resolved analytically, the following approximation is applied:

$$\int_0^{\Delta x} \nabla \mu_\ell dx \approx \Delta \mu_\ell \tag{14}$$

where $\Delta \mu_l$ is the chemical potential difference between two phases. According to the mass-transfer theory, the flux J_i can be expressed as

$$J_i = c_t^V K_i^{OV} (y_i^* - y_i) \tag{15}$$

where y_i^* $(=M_i x_i)$ is the vapor mole fraction of component i that is in equilibrium with the liquid phase. The component i in Eq. 15 can be either a light component ($i = l$) or a heavy component ($i = h$). Inserting Eq. 15 into Eq. 4 generates the following equation:

$$J_d = \frac{c_t^V K_\ell^{OV} (M_\ell x_\ell - y_\ell)}{x_\ell} - \frac{c_t^V K_h^{OV} (M_h x_h - y_h)}{x_h} \tag{16}$$

By combining Eqs. 13, 14, and 16, Θ_p can be finally expressed as

$$\Theta_p = \frac{c_t^V x_\ell \Delta \mu_\ell}{T} \left[\frac{K_\ell^{OV} a (M_\ell x_\ell - y_\ell)}{x_\ell} - \frac{K_h^{OV} a (M_h x_h - y_h)}{x_h} \right] \tag{17}$$

When the liquid and vapor phases are mixed completely, the compositions in the liquid are uniform, so Eq. 17 can be directly used to calculate the EGR resulting from the mass transfer for a small-scale stage. However, for the large-scale stage, there are different compositions on different parts of the stage. Equation 17 can be applied only to calculate the EGR resulting from mass transfer for each pool, Θ_p. Thus, the EGR per tray resulting from mass transfer in the stage (Θ_l) can be obtained using the following equation:

$$\Theta_\ell = \sum_{p=1}^{n} \Theta_p \tag{18}$$

where n is the number of the mixing pools.

The EGR arising from the temperature gradient is normally neglected in the case of liquid and vapor phases being mixed completely.[3] However, because the temperature gradient on an industrial-scale tray may be considerable, the EGR resulting from the temperature gradient should be analyzed carefully. The EGR comes from the thermal conduction that takes place mainly in the gas and liquid bulks, thus

$$\Theta_q = \int_v \sigma_q \, dv = \int_{v^V} \sigma_q \, dv + \int_{v^L} \sigma_q \, dv = \Theta_q^V + \Theta_q^L \tag{19}$$

To calculate σ_q, the profile of temperature gradients on the industrial tray should be known. The temperature gradients are generated mainly along two directions[13]: the vertical direction, in which gas bubbles pass through the liquid layer, producing a temperature gradient of $\bigtriangledown T_{ver}$; and the horizontal direction, in which the liquid flows, generating a temperature gradient of $\bigtriangledown T_{hor}$. According to the law of vector addition, the square of magnitude of the total temperature gradient can be written as

$$|\nabla T|^2 = |\nabla T_{ver}|^2 + |\nabla T_{hor}|^2 \tag{20}$$

By introducing Eq. 9 and Eq. 20 into Eq. 19, ${\Theta_q}^V$ can be obtained as

$$\begin{aligned} \Theta_q^V &= \int_{v^V} \sigma_q dv = \int_{v^V} \lambda^V \left(\frac{|\nabla T_{ver}|}{T} \right)^2 dv + \int_{v^V} \lambda^v \left(\frac{|\nabla T_{hor}|}{T} \right)^2 dv \\ &= \int_o^{h_f} \lambda^V \left(\frac{|\nabla T_{ver}|}{T} \right)^2 e A_a dh_f + \int_0^D \lambda^V \left(\frac{|\nabla T_{hor}|}{T} \right)^2 e A_v dl_f \\ &= \lambda^V \left(\frac{|\nabla T_{ver}|}{T} \right)^2 ev + \lambda^V \left(\frac{|\nabla T_{hor}|}{T} \right)^2 ev \\ &= \lambda^V \frac{|\nabla T_{ver}|^2 + |\nabla T_{hor}|^2}{T^2} G \end{aligned} \tag{21}$$

Similarly, the EGR in the liquid bulk (${\Theta_q}^L$) can also be formulated as

$$\Theta_q^L = \lambda^L \frac{|\nabla T_{ver}|^2 + |\nabla T_{hor}|^2}{T^2} L \tag{22}$$

Given that plug flow conditions are assumed for the liquid phase, $\bigtriangledown T_{ver}$ and $\bigtriangledown T_{hor}$ are constants[13] that can be expressed as

$$\nabla T_{ver} = \frac{\Delta T_{ver}}{\Delta h_f} \tag{23}$$

$$\nabla T_{hor} = \frac{\Delta T_{hor}}{\Delta l_f} \tag{24}$$

where h_f is the froth height and l_f is the distance from the inlet to the vertical section. Provided that the coefficient of heat conductivity λ on each stage is constant, the EGR for a stage resulting from $\bigtriangledown T$ can be written as

$$\Theta_q = \frac{(\lambda^V G + \lambda^L L)}{T^2} \left(\left| \frac{\Delta T_{ver}}{\Delta h_f} \right|^2 + \left| \frac{\Delta T_{hor}}{\Delta l_f} \right|^2 \right) \tag{25}$$

For the tray having a diameter < 0.8 m, the flow of liquid and gas could be considered to be completely mixed, so that $\nabla T_{hor} = 0$ and Θ_q can be simplified as

$$\Theta_{q,s} = \left|\frac{\Delta T_{ver}}{\Delta h_f}\right|^2 \frac{(\lambda^V G + \lambda^L L)}{T^2} \tag{26}$$

Equations 17, 18, 25, and 26 are the working equations for the calculation of the local EGR per tray.

Simulation of the Distillation Process

At present, one of the many efforts to develop the distillation process simulation is to replace the equilibrium stage model with the nonequilibrium stage model. In this work, the MEF model[6] is adopted and modified to coordinate with the nonthermodynamic energy analysis. Feed streams and heat fluxes are contained in each stage, as shown in Figure 2, and the METSH equation group is listed as follows:

Total Material Balance (M)

$$F_j + L_{j-1} + G_{j+1} - (L_j + U_j) - (V_j + G_j) = 0 \tag{27a}$$

Component Material Balance (M_i)

$$F_j x_{i,j}^F + L_{j-1} x_{i,j-1} + G_{j+1} y_{i,j+1} - (L_j + U_j) x_{i,j} - (V_j + G_j) y_{i,j} = 0 \tag{27b}$$

Phase Equilibrium (E)

$$y_{i,j}^* = M_{i,j} x_{i,j} \tag{28}$$

Vapor Tray Efficiency Equations (T)

$$E_{i,j}^{MV} = \frac{y_{i,j} - y_{i,j+1}}{y_{i,j} - y_{i,j+1}} \tag{29}$$

Summation Equations (S)

$$\sum_{i=1}^{c} x_{i,j} - 1 = 0 \tag{30a}$$

$$\sum_{i=1}^{c} y_{i,j} - 1 = 0 \tag{30b}$$

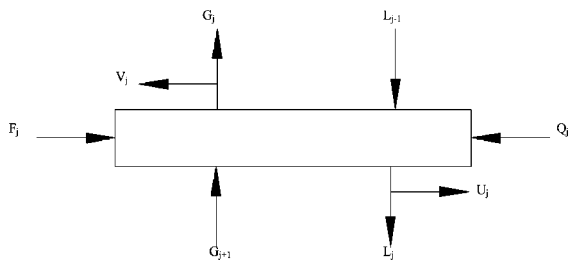

Figure 2. Distillation process simulation.

Heat Balance (H)

$$F_j H_j^F + G_{j+1} H_{j+1}^V + L_{j-1} H_{j-1}^L - (V_j + G_j) H_j^V - (L_j + U_j) H_j^L + Q_j = 0 \tag{31}$$

where the tray efficiency $E_{i,j}^{MV}$ is determined by the performance of each tray. For the industrial-scale tray as shown in Figure 1, the integration of the material balance in each pool may be arranged to give the following vapor Murphree point efficiency[6]:

$$(y_{i,j}^P - y_{i,j+1}^P) = E_{i,j}^P (y_{i,j}^{*,P} - y_{i,j+1}^P) \tag{32}$$

$$E_{i,j}^P = 1 - \exp(-N_{i,j}^{OV}) \tag{33}$$

$$N_{i,j}^{OV} = c_t^V K_{i,j}^{OV} a A_a h_f / G_j \tag{34}$$

In addition, the correlation between point efficiency ($E_{i,j}^P$) and tray efficiency ($E_{i,j}^{MV}$) can be written as[14]

$$E_{i,j}^{MV} = \left(M_{i,j}\frac{G_j}{L_j}\right)^{-1}\left[\left(1 + \frac{E_{i,j}^P M_{i,j} G_j}{n L_j}\right)^n - 1\right] \tag{35}$$

where n is the number of pools. If $n = 1$, the tray efficiency is equal to point efficiency and the liquid phase is completely mixed. If $n = \infty$, the liquid phase is at a state of plug flow and the expression for the Murphree tray efficiency is[15]

$$E_{i,j}^{MV} = \left(M_{i,j}\frac{G_j}{L_j}\right)^{-1} \exp\left(E_{i,j}^P M_{i,j}\frac{G_j}{L_j} - 1\right) \tag{36}$$

With the help of Eqs. 32–36 for calculating the $E_{i,j}^{MV}$values, the METSH equation group (Eqs. 27–31) can be solved to yield the stage flow rates, compositions, and temperatures that are requisite parameters for the calculation of the EGR in an industrial-scale column.

Calculation Procedure

The distillation column for the separation of benzene and toluene is studied as the model system and the column specifications, such as stage numbers and feed stages, are listed in Table1.

The model equations, mainly the METSH equation group, are solved using the tridiagonal matrix method. A computer program is developed to implement the stage model described above. Different flow patterns on the trays are considered: completely mixed flow, plug flow, and intermediate cases.

The physical properties of pure components are calculated using the correlations from *Lange's Handbook of Chemistry*[16] and the mixture properties are calculated according to the methods recommended in the *Petrochemical Engineering Design Handbook*.[17] The phase equilibrium is computed using the data from Gmehling et al.[18] The virial and the Wilson equations are applied for the gas phase and liquid phase, respectively. The mass-transfer coefficients for the sieve tray are predicted using the method proposed by

Table 1. Column Specification for the Separation of Benzene–Toluene

Stages number	48	Feed stage	23
H_t, m	0.5	Diameter, m	2.6
Weir length, m	1.56, 1.82, 2.08	Weir height, m	0.02, 0.05, 0.08
A_d/A_t	0.65, 0.8, 0.95	X_1 at the feed	0.44
X_1 at the bottom	<0.02	X_1 at the top	>0.98

AIChE,[19] whereas the Richard[20] method is applied to the V-1 valve tray. The approach to calculate the overall mass transfer is recommended by multicomponent mass transfer.[6] The top condenser is assumed to be at 101,325 Pa and the pressure drop is calculated according to the method recommended in *Perry's Chemical Engineering's Handbook*.[21]

Results and Discussion

Because the model introduced herein can be adopted not only to simulate the distillation process but also to analyze the energy consumption with nonequilibrium thermodynamics, the stage compositions, temperature, pressure, liquid and vapor streams, tray efficiency, and EGR for each stage could be obtained from this model. Three aspects influenced the EGR results: the tray structure, operation parameters, and physical properties. Herein, we mainly aim at determining the effects of tray structure and operating parameters on the EGR.

Comparison between exergy analysis and nonequilibrium thermodynamic analysis

To evaluate the validity of the model, the EGR results calculated by the exergy analysis and nonequilibrium thermodynamic analysis are compared, as shown in Figure 3. The method of calculating the EGR by exergy analysis is given in the Appendix. It is found that the EGR from nonequilibrium thermodynamic analysis varies according to the same trend as that from exergy analysis, even though the difference between these two methods of analysis is still considerable. Other researchers[22] also found such results, but few of them tried to explore the reasons for such outcomes.

Exergy is the state function of the studied thermodynamic system (both the liquid and vapor on the tray). When the system changes from one state to another, the exergy loss occurs as a result of all the irreversible phenomena taking place on the trays, such as mass transfer, heat transfer, pressure drop, phase mixing, and so on. Therefore, the exergy loss calculated from exergy analysis is a kind of "black box" value, which means the indistinguishability of contribution sources of the total exergy loss. On the contrary, nonequilibrium thermodynamic analysis is performed to evaluate the EGR process (or exergy loss) directly from all possible driving forces of the irreversible phenomena, such as the concentration gradient or chemical potential gradient of the mass transfer and the temperature gradient of the heat transfer. It reveals how and to what extent the various phenomenal driving forces contribute to the EGR process and indicates the detailed energy consumption information that is useful for modification of the distillation process. Because the distillation process usually involves mass and heat transfers, and other minor driving forces are neglected, it is rational that the calculated EGR process from nonequilibrium thermodynamics is slightly smaller than that from exergy analysis. In addition, the discrepancy between the two analyses may also partly be explained by the inaccurate estimation of the excess entropy and enthalpy in the exergy analysis. The excess entropy and enthalpy, the required data for energy calculation of a mixture, have to be obtained from the commonly used empirical EoS (equation of state) and G^E (excess Gibbs energy) models, which affect the accuracy of the calculated data. Thus, nonequilibrium thermodynamic analysis is a comparatively simple and straightforward method that avoids calculating the excess entropy and enthalpy and enables one to evaluate, separately, the contributions from various phenomenal driving forces to the EGR.

Therefore, it is concluded that nonequilibrium analysis is a more feasible and applicable alternative for the distillation process. It could be conveniently used to evaluate the effects of the tray structure and operation parameters on the EGR, which could not be performed using exergy analysis.

EGR resulting from the temperature gradient

In this model, the EGR arising from the temperature gradient is calculated based on the assumption of vapor and liquid flow in the plug pattern. As shown in Figure 4, although the square of the temperature gradients is considerable, the EGR resulting from the temperature gradient is not comparable to the total EGR even in the industrial-scale stages with a diameter of 2.6 m. It could be rationalized that the internal heat flux is comparatively small, whereas the external heat loss to the surroundings is neglected in the model. However, both of the internal and external heat fluxes may be accumulated to generate larger temperature gradients in an actual separation tower than in the model. The calculation here could be used for reference.

Overall mass-transfer coefficient

In all nonequilibrium thermodynamic models, the mass-transfer coefficient plays an important role. In this model, the overall mass-transfer coefficient is introduced to calculate the tray efficiency and EGR.

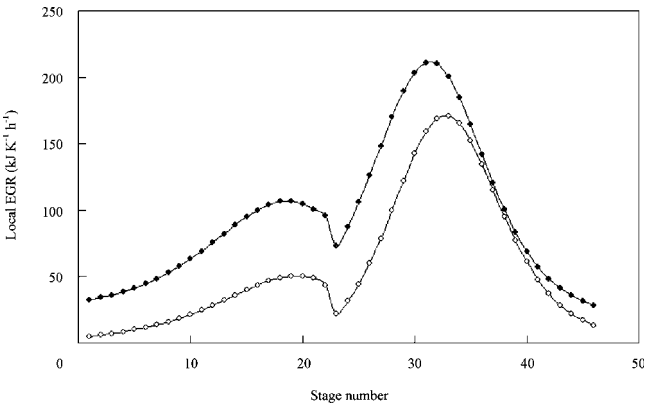

Figure 3. Local EGRs calculated by the nonequilibrium analysis (○) and the exergy analysis (●).

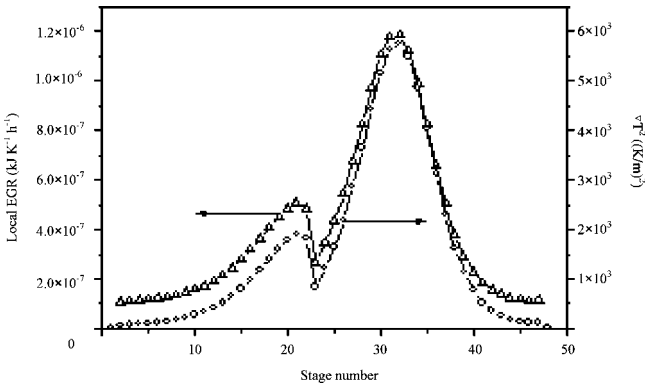

Figure 4. Local EGRs arising from the temperature gradients (△) and the square of temperature gradients ∇T^2 (○).

The overall mass-transfer coefficient accounts for the mass transfers both in the vapor and liquid phases and could simplify the simulation procedure and dramatically reduce the computation time.[23] In this study, because the overall mass-transfer coefficient can be uniquely defined for binary systems, the processor EGR calculation herein is accurate and can be taken as the preparatory estimation for the case of multicomponent systems in the future.

Different types of trays have different correlations of mass-transfer coefficients. In the present work, two primary trays are studied: sieve tray and Glitsch V-1 valve tray. For the sieve tray, the mass-transfer coefficient data are obtained from the AIChE method[19] and those for the valve tray are from Richard.[20] Under the assumption that the pressure drops per tray of two types are identical, the calculation shows that the mass-transfer coefficients of V-1 valve trays almost double those of the sieve trays, leading to the different local EGR values of two types, as shown in Figure 5. The EGR values of the valve tray are higher than those of the sieve tray in the middle section (near the feeding stages, trays 18–32) and become lower in the bottom section (trays 33–48). The higher EGR values near the feeding stages are primarily attributed to the higher mass-transfer coefficients that induce greater mass flux because the chemical potential gradients are almost unchanged. Nevertheless, in the bottom section

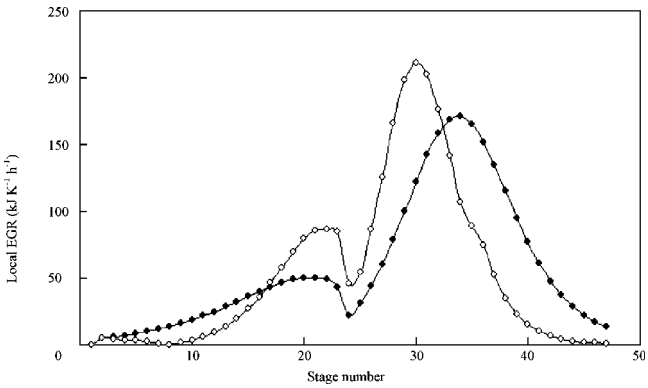

Figure 5. Local EGRs for V-1 valve tray (○) and sieve tray (●).

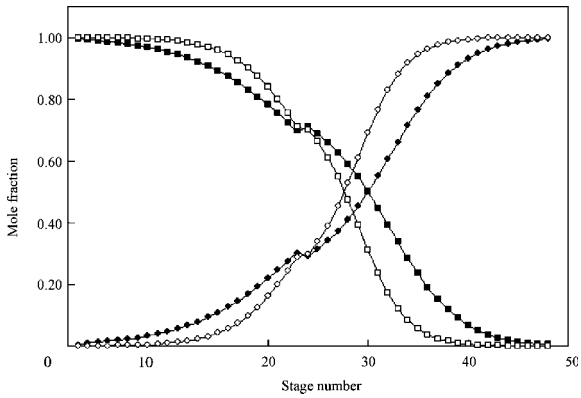

Figure 6. Vapor mole fractions of benzene on each stage for V-1 valve tray (□) and sieve tray (■); liquid mole fractions of toluene on each stage for V-1 valve tray (○) and sieve tray (●).

the chemical potential gradients are substantially reduced and, accordingly, the EGR values are greatly reduced for the valve tray.

Figure 6 presents the concentrations on each stage. It is found that the main mass-transfer region is in the middle section and the concentration profiles between the two tray columns differ considerably. Because a high mass-transfer coefficient determines high tray efficiency, fewer stages are required for the valve column to fulfill the specified separation duty. In the case studied here, only 32 pieces of valve trays are required compared with 48 pieces of sieve trays. Another difference between two columns is the heater supply, 0.242E8 kJ/h^{-1} at 390.32 K for a sieve column and 0.241E8 kJ/h^{-1} at 388.21 K for the valve column. This result can serve as the basis for economic analysis.

Flow patterns

The vapor and liquid flow patterns on the tray dramatically affect the vapor and liquid distribution, pressure drop, tray efficiency, and so on. Numerous investigations on this aspect

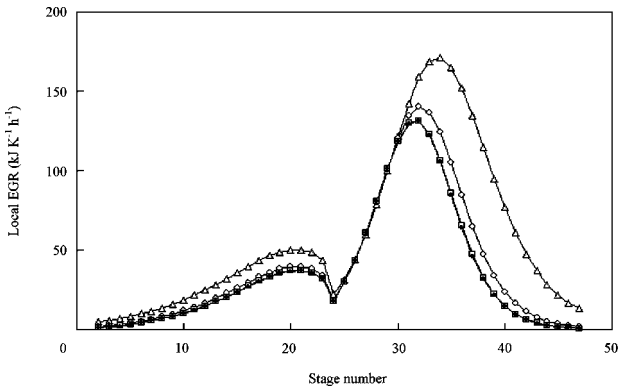

Figure 7. Local EGRs under different mixing conditions.

Completely mixed (△), 5 compartments (○), 100 compartments (□), plug flow (●).

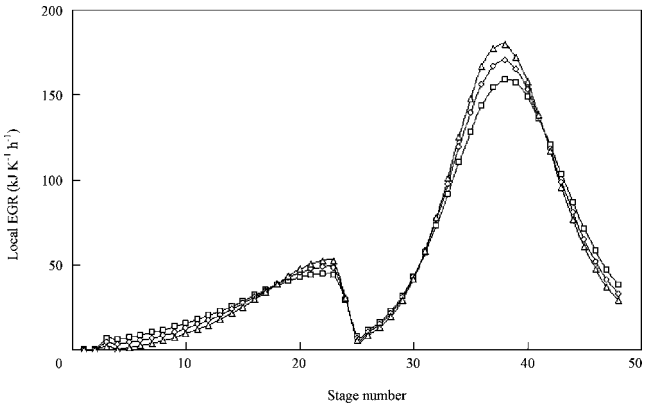

Figure 8. Local EGRs with different weir heights: 0.02 m (□), 0.05 m (○), 0.08 m (△).

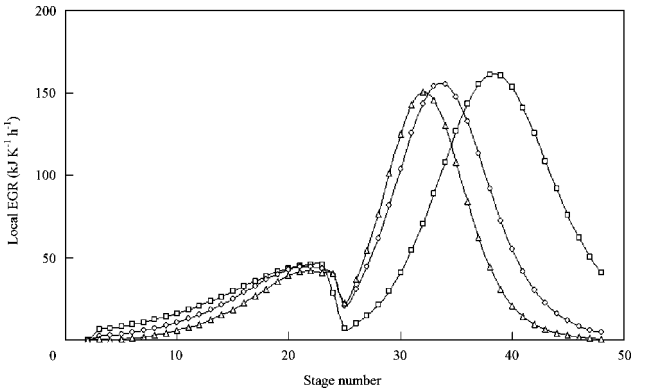

Figure 10. Local EGRs with different active areas: A_a/A_t = 0.95 (△); A_a/A_t = 0.80 (○); A_a/A_t = 0.65 (□).

have been carried out and some excellent trays were developed to improve the flow patterns.

It is believed that the flow patterns of vapor and liquid on small trays, with diameter < 0.8 m, have little influence on the EGR process because vapor and liquid are usually close to the state of being mixed completely. However, there are different behaviors on an industrial-scale tray. In this work, an industrial-scale tray with diameter 2.6 m is selected to study the effect of the flow pattern on the EGR. It is the first time that the mixing pool model is applied to compute the EGR. Four conditions are assumed: 1 compartment (complete mixing), 5 compartments, 100 compartments, and infinite compartments (plug flowing). Complete mixing represents the severe back-mixing condition. It leads to the increasing liquid volume and pressure drop on a tray, which further result in low tray efficiency, high chemical potential gradient, and thus increased EGR, as shown in Figure 7. The EGR difference between the 100 compartments and plug flow is very slight, whereas the EGR of 5 compartments is a fair approximation to that of plug flow. So a suitable number of pools will correctly evaluate the influence of the back-mixing condition on the performance of an industrial-scale tray, and the better flow pattern requires a larger number of pools.

Tray structure

Our previous work[4] investigated the dependency of EGR on the tray structure. However, the analysis and conclusion in the previous work were based on a simple but awkward assumption that the values of tray efficiency were artificially set to be constant. This assumption deviates from the real case. In this work, the multicomponent efficiency is calculated based on the overall mass-transfer coefficient, so that more rigorous results can be obtained to analyze the influence of tray structure on the industrial-scale tray column.

The tray structure mainly influences the pressure drop and the mass-transfer efficiency. Because the weir height, weir length, and active area, being expressed in the universal correlations such as those of the AIChE method,[19] are the key tray structure parameters that influence the mass transfer and the pressure drop, it is important and interesting to evaluate the influence of these parameters on the EGR process.

The higher weir height induces the increase of both the tray efficiency and the pressure drop. On the one hand, the high tray efficiency enlarges the mass flux, leading to the increase of the local EGRs in the middle section, given that the chemical potential gradients are nearly unchanged. How-

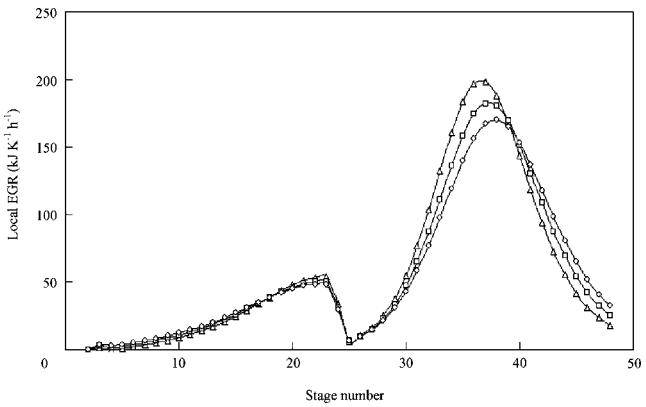

Figure 9. Local EGRs with different weir lengths: 1.56 m (△), 1.82 m (○), 2.08 m (□).

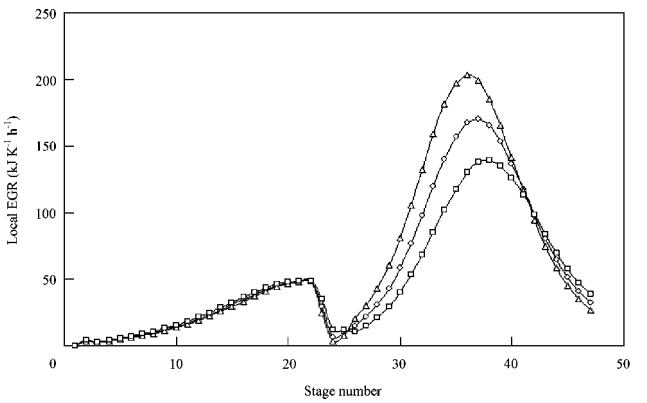

Figure 11. Local EGRs with different locations of heat exchange in the stripping section.

Heat fed in the tray No. 25 (△), no side heat exchange (○), heat taken out of the tray No. 25 (□).

Table 2. Simulation Results with Different Heat Exchange Duty

	Case I	Case II	Case III	Case IV	Case V
Heat exchanger duty, kJ h^{-1}	—	0.2E7	−0.2E7	0.2E7	−0.2E7
Heat exchanger temperature, K	—	368.23	369.90	354.76	355.08
Exchanger location	—	25	25	6	6
Reboiler duty, kJ h^{-1}	0.244E08	0.224E8	0.262E8	0.244E8	0.244E8
Reboiler temperature, K	393.84	393.95	393.70	393.99	393.61
Condenser duty, kJ h^{-1}	−0.199E8	−0.199E8	−0.199E8	−0.219E8	−0.179E8
Condenser temperature, K	353.43	353.42	353.44	353.39	353.49
Local EGR, kJ K^{-1} h^{-1}	Figures 11, 12	Figure 11	Figure 11	Figure 12	Figure 12
Total EGR, kJ K^{-1} h^{-1}	2574.90	2868.61	2292.14	2974.99	2183.18
X_1 at the top	0.9915	0.9919	0.9909	0.9934	0.9885
X_2 at the bottom	0.9939	0.9956	0.9915	0.9961	0.9901

ever, in the bottom section (trays 40–48), the local EGRs dramatically decrease because of the reduction of the potential gradients. On the other hand, the increased pressure drop always causes the increase of the local EGR. As a result, the combined effect of a higher weir is to increase the total EGR of the whole distillation process, as shown in Figure 8.

The longer weir length is helpful in reducing the liquid crest over the weir at a definite liquid flow rate, which implies that the tray pressure drop and tray efficiency decrease accordingly. Such behavior is contrary to that of weir height. Figure 9 shows that an increase in the weir length results in a reduction of the local EGRs in the middle section (trays 20–40) and thus the reduction of the total EGR.

The increased active area will noticeably reduce the total EGR, as shown in Figure 10. This is mainly attributed to the simultaneous actions of the reduced pressure drop and the increased tray efficiency. Even though the local EGRs in the middle section (trays 20–32) increase to some extent, the significant reduction of the local EGRs in the bottom section (trays 32–48) as well as the appreciable reduction in the top section (trays 1–20) cause the noticeable decrease of the total EGR.

The analysis above denotes that it is the key strategy of tray structure design to reduce pressure drop and enhance tray efficiency simultaneously for the sake of reducing the EGR.

Operation parameter: side heat exchanger

For all routine operating parameters, such as reflux ratio and feed temperature, the calculated results here are similar to the conclusions reported by Liu et al.[4] Our attention here is focused on evaluating how the addition of side heat exchangers influences the process EGR. This is because the design of side heat exchanges nowadays becomes simple, whereas the increasing energy crisis compels a reduction in energy consumption. If the investment on the added heat exchanges can balance the bonus from energy-saving, such modification will become realistic. In addition, our effort for doing this is also of scientific significance. The side heat exchanger locations have different influences on the EGR, so our aim here is to evaluate such influences.

When the heat is fed into the stripping section (Case II), the local EGRs on stages below the position of the heat exchanger (trays 24–40) noticeably increase, while slightly decreasing in the bottom section (trays 40–48), as shown in Figure 11. The reason is that the additional heat accelerates the mass transfer on stages below the heat exchanger, whereas the chemical potential gradients are almost kept invariable on trays 24–40 and reduced on trays 24–40. Although the total EGR of Case II is greater than that of Case I, the component purity increases at a certain extent and the reboiler duty is decreased accordingly, as shown in Table 2. When the heat is removed from the stripping section (Case III), opposite results to those of Case II are obtained.

For the same reason as above, when the heat is fed into the enriching section (Case IV), the profile of the local EGRs is similar to that of Case II, as shown in Figure 12. With respect to Case V, the results are contrary to those of Case IV.

From the preceding analysis, it is concluded that adding a second reboiler at the stripping section (Case II) results in higher separation efficiency and lower reboiler duty, although a small increase of total EGR is generated. Case II can be regarded as a comparatively effective modification strategy.

Conclusions

A nonequilibrium thermodynamic model that is capable of simulating the industrial distillation process, while simultaneously analyzing the energy consumption, is developed and tested using the benzene–toluene binary distillation system. The calculation of the EGR process is improved by introducing the overall mass-transfer coefficient into the model. The introduced overall mass-transfer coefficient becomes the con-

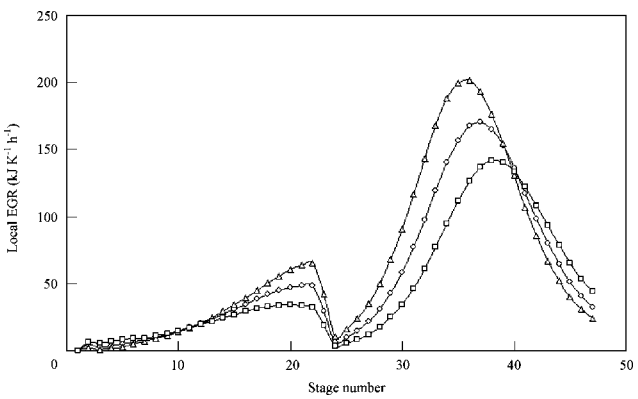

Figure 12. Local EGRs with different locations of heat exchange in the enriching section.

Heat fed in the tray No. 6 (△), no side heat exchange (○), heat taken out of the tray No. 6 (□).

venient and effective linkage between process simulation and EGR calculation in the model.

It is shown that the EGR process calculated by the model is similar to that using exergy analysis, indicating the feasibility of the model. Nonequilibrium thermodynamic calculation has a rigorous advantage over exergy analysis because the former can be readily used to examine the influences of the tray type, tray structure, and flow patterns on energy consumption. No matter what kinds of tray type and tray structure are selected, the calculation shows that the local EGR increases with increasing mass flux and pressure drop on each tray. However, large mass flux not only can enhance tray efficiency, which is helpful to the separation duty, but also can dramatically reduce the chemical potential gradients that are proportional to the EGR. Therefore, as a general effect, high tray efficiency and small pressure drop can always considerably reduce the total EGR of the whole distillation process. With respect to the exact effects of the tray structure on the EGR process, the calculation shows that the total EGR decreases with decreasing weir height and increasing active area and weir length. This information can be used to aid the design of tray structure.

The EGR process of the industrial-scale tray is studied for the first time. It is found that improvement of vapor and liquid flow patterns can appreciably enhance tray efficiency and reduce tray pressure drop, causing an effective decrease in the EGR process. The heat duty, as one of the most important operating parameters, should also simultaneously be taken into account. The calculations indicate that the most effective strategy is to add a second reboiler at the stripping section when renovating an old distillation process. It is believed that the nonequilibrium process simulation and energy analysis model can provide a powerful tool for analyzing, optimizing, and designing distillation processes. More efforts on extending the model to other distillation systems, especially multicomponent systems, are now under way in our laboratory.

Acknowledgments

The authors are grateful for the financial support from National 985 Project of China and National Natural Science Foundation of China (Grant 20576050).

Notation

a = interfacial area per froth volume, m^2/m^3
A_a = tray active area, m^2
A_t = tray traverse section area, m^2
A_v = froth vertical section area, m^2
c_t = total concentration, mol/m^3
e = vapor volume fraction
E = tray efficiency
Ex = exergy, kJ/mol
F = flow rate of feed stream, mol/h
G = vapor flow rate, mol/h
h_f = froth height, m
H = enthalpy, kJ/mol
J = diffusion flux, mol m^{-2} h^{-1}
K = mass-transfer coefficient, m/s
l = phenomenological coefficient
L = liquid flow rate, mol/h
S = entropy, kJ K^{-1} mol^{-1}
T = mean temperature on the tray, K
∇T = temperature gradient, K/m
U = liquid flow rate of side stream, mol/h
v = froth volume, m^3
V = vapor flow rate of side stream, mol/h
x = liquid mole fraction
y = vapor mole fraction

Greek letters

λ = heat conductivity, W K^{-1} m^{-1}
μ = chemical potential, kJ/mol
σ = entropy generation rate per unit volume, kJ K^{-1} m^{-3} h^{-1}
Θ = entropy generation rate per unit stage, kJ K^{-1} h^{-1}
δ = Krönecker operator

Superscripts

F = feed stream
I = interface
L = liquid
MV = Murphree vapor phase
OV = overall vapor phase
P = point
V = vapor

Subscripts

h = heavy component
hor = horizontal
i = component number
j = tray number
k = random stream
l = light component
n = mixing pool number
ver = vertical

Literature Cited

1. Seader JD, Henley EJ.*Separation Process Principles*. New York: Wiley; 1998.
2. Ray S, Sengupta SP. Irreversibility analysis of a sieve tray in a distillation column. *Int J Heat Transfer*. 1996;39:1535–1542.
3. Ratkj SK, Sauar E, Hansen EM, Lien KM, Hafskjoild B. Analysis of EGRs for design of distillation columns. *Ind Eng Chem Res*. 1995; 34:3001–3007.
4. Liu QL, Li P, Xiao J, Zhang ZB. A new method for design an energy-saving tray and its hydrodynamic aspects: Model development and simulation. *Ind Eng Chem Res*. 2002;41:285–292.
5. Tonder D, Kvaalen E. Equipartition of entropy production. An optimality criterion for transfer and separation processes. *Ind Eng Chem Res*. 1987;26:50–56.
6. Taylor R, Krishna R.*Multicomponent Mass Transfer*. New York: Wiley; 1993.
7. Krishnamurty R, Taylor R. A nonequilibrium stage model of multicomponent separation processes. *AIChE J*. 1985;31:449–465.
8. Krishna R. A simplified mass transfer analysis for multicomponent condensation (Letter). *Heat Mass Transfer*. 1979;6:439.
9. Taylor R, Smith LW. On some explicit approximate solutions of the Maxwell–Stefan equations for the multicomponent film model. *Chem Eng Commun*. 1982;14:361.
10. Kooijman HA, Taylor R. Modelling mass transfer in multicomponent distillation. *Chem Eng J*. 1995;57:177–188.
11. Niels P, Muller HS. An overall rate-based stage model for cross flow distillation columns. *Chem Eng Sci*. 2000;55:2513–2528.
12. Forland KS, Forlad T, Ratkje SK. *Irreversible Thermodynamics: Theory and Application*. New York:Wiley; 1994.
13. Zhou Z, Liang YC, Zhang ZB. A new method for design an energy-saving tray and its hydrodynamic aspects: Temperature distribution and efficiency of deflected tray-95. *Ind Eng Chem Res*. 2003;42: 2219–2222.
14. Gautreaax MF, O'Connel HE. Effect of length of liquid path on plate efficiency. *Chem Eng Prog*. 1955;51:232–237.
15. Toor HL. Prediction of efficiencies and mass transfer on a stage with multicomponent system. *AIChE J*. 1964;10:545–547.

16. Dean JA. *Lange's Handbook of Chemistry*. New York:McGraw-Hill; 1972.
17. Wang SH. *Petrochemical Engineering Design Handbook*. Beijing:-Chemical Industry Publishing; 2002.
18. Gmehling J, Onken U, Arlt W. *Vapor–Liquid Equilibrium Data Collection*. Frankfurt/Main, Germany: Dechema; 1977.
19. American Institute of Chemical Engineers (AIChE). *Bubble Tray Design Manual: Prediction of Fractionation Efficiency*. New York: AIChE; 1958.
20. Scheffe RD, Weiland RH. Mass-transfer characteristics of valve trays. *Ind Eng Chem Res*. 1987;26:228–236.
21. Perry RH, Green DW. *Perry's Chemical Engineering's Handbook*. New York: McGraw-Hill; 1997.
22. Zemp RJ, de Faria SHB, de L'Oliveira Maia M. Driving force distribution and exergy loss in the thermodynamic analysis of distillation columns. *Comput Chem Eng*. 1997;21:523–528.
23. Pescarini MH, Barros AAC, Wolf-Maciel MR. Development of a software for simulating separation processes using a nonequilibrium stage model. *Comput Chem Eng*. 1996;20:279–284.
24. Walas SM. *Phase Equilibria in Chemical Engineering*. Stoneham, MA: Butterworth; 1985.

Appendix: Exergy Analysis for the Estimation of the EGR

Our main interest is the irreversibility on the trays; the exergy loss on tray j (Ex_j^{loss}) is calculated with an exergy balance over the tray (see Figure 2 for the symbols and numbers):

$$Ex_j^{loss} = F_j Ex_j^F + G_{j+1} Ex_{j+1}^V + L_{j-1} Ex_{j-1}^L - (V_j + G_j) Ex_j^V - (L_j + U_j) Ex_j^L + Q_j \left(1 - \frac{T_0}{T_j}\right) \quad (A1)$$

The exergy of one section Ex_k is calculated by

$$Ex_k = H_k - T_0 S_k \quad (A2)$$

where $T_0 = 298.15$ K and subscript k denotes a random stream. Exergy loss and EGR in distillation are related to each other by the Gouy–Stodola theorem:

$$\Theta_j = Ex_j^{loss}/T_0 \quad (A3)$$

The entropy and enthalpy of pure gas at $T_0 = 298.15$ K and $P_0 = 101{,}325$ Pa are arbitrarily assumed to be zero. The calculation methods of the absolute entropy and enthalpy needed to calculate the exergy values are obtained from Walas.[24] For nonideal vapor and liquid mixtures the virial expression and Wilson equation are used, respectively, to estimate the excess entropy and enthalpy.

Manuscript received Nov. 30, 2005, and revision received Sept. 24, 2006